

ISSN: 0256-307X

# 中国物理快报

# Chinese Physics Letters

Volume 28 Number 3 March 2011

A Series Journal of the Chinese Physical Society  
Distributed by IOP Publishing

Online: <http://iopscience.iop.org/cpl>  
<http://cpl.iphy.ac.cn>

**CHINESE PHYSICAL SOCIETY**  
Institute of **Physics** PUBLISHING

JOURNAL FOR AUTHORS  
— CHINESE PHYSICS LETTERS

## A New Car-Following Model with Consideration of Driving Resistance \*

LI Chuan-Yao(李传耀)<sup>1</sup>, TANG Tie-Qiao(唐铁桥)<sup>1,2\*\*</sup>, HUANG Hai-Jun(黄海军)<sup>2</sup>,  
SHANG Hua-Yan(尚华艳)<sup>3</sup>

<sup>1</sup>School of Transportation Science and Engineering, Beijing University of Aeronautics and Astronautics, Beijing 100191

<sup>2</sup>School of Economics and Management, Beijing University of Aeronautics and Astronautics, Beijing 100191

<sup>3</sup>Information College, Capital University of Economics and Business, Beijing 100070

(Received 8 June 2010)

Based on the effects of driving resistance on car movement, we develop a new car-following model. The simulation results show that our model can describe the kinetic property of each car during the processes of starting and braking, however the braking process will be postponed and a prominent wavefront will appear during the braking process. With the increase in driving resistance, a car's movement will become more stable during the whole process, the headway of each car will increase and the wavefront will become more prominent. In addition, our model can reproduce the evolution of a small perturbation.

PACS: 89.40.-a, 45.70.Vn

DOI: 10.1088/0256-307X/28/3/038902

So far, serious traffic problems have attracted scholars to develop many traffic flow models to study various complex traffic phenomena.<sup>[1,2]</sup> Among the existing traffic flow models, the cellular automaton (CA) model can describe the micro property of car motion, so it was used to explore some microscopic phenomena of traffic flow.<sup>[3-7]</sup> In fact, the car-following model can also describe the micro phenomena of traffic flow. Pipe<sup>[8]</sup> proposed the first car-following model and scholars have extended this model.<sup>[9-12]</sup> Since the car-following model consists of a series of ordinary differential equations and is restricted by the performance of computers, few car-following models were developed from 1970s to 1980s. With the development of computers, scholars later proposed many new car-following models from different perspectives.<sup>[13-28]</sup> These car-following models can describe many complex traffic phenomena, but they cannot be employed to explore the effects of driving resistance on traffic flow. In a real traffic system, driving resistance affects car motion. Based on the property of the driving resistance, in this Letter we develop a new car-following model and use it to explore the dynamic property of each car during the processes of the starting and braking and the evolution of a small perturbation.

The car-following model on a single lane can be reduced as follows:<sup>[1]</sup>

$$\frac{dv_n}{dt} = f(v_n, \Delta x_n, \Delta v_n), \quad (1)$$

where  $v_n$  is the  $n$ th car's velocity,  $f(\cdot)$  is the stimulus function determined by the headway  $\Delta x_n = x_{n+1} - x_n$  ( $x_n$  is the  $n$ th car's position), the relative velocity  $\Delta v_n = v_{n+1} - v_n$  and the velocity  $v_n$  (see Fig. 1).

In order to further study traffic flow, scholars later developed some extended models to consider multi headways:<sup>[15,16,19,20]</sup>

$$\frac{dv_n}{dt} = f(v_n, \Delta x_n, \Delta x_{n+1}, \dots, \Delta x_{n+m}, \Delta v_n), \quad (2)$$

where  $\Delta x_{n+i} = x_{n+i+1} - x_{n+i}$ . Zhao and Gao<sup>[22]</sup> found that collisions will occur under certain conditions when the full velocity difference (FVD) model<sup>[17]</sup> is used to describe traffic flow, thus they developed a new car-following model which considered the acceleration of the leading car:

$$\frac{dv_n}{dt} = f(v_n, \Delta x_n, \Delta v_n, dv_{n+1}/dt). \quad (3)$$

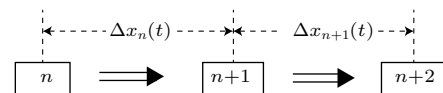


Fig. 1. Scheme of the car-following model.

To further enhance the stability of traffic flow, Wang *et al.*<sup>[23]</sup> proposed a multiple velocity difference model as follows:

$$\frac{dv_n}{dt} = f(v_n, \Delta x_n, \Delta v_n, \Delta v_{n+1}, \dots, \Delta v_{n+k}), \quad (4)$$

where  $\Delta v_{n+i} = v_{n+i+1} - v_{n+i}$ .

Although the above models can describe some complex phenomena, they cannot directly be used to study the effects of driving resistance on car-following behavior. In fact, each car has a driving resistance that will affect its following behavior, thus Yu<sup>[29]</sup> pointed out that the drivers should consider driving resistance during the driving process. In a real traffic

\*Supported by the Program for New Century Excellent Talents in University under Grant No NCET-08-0038, the National Natural Science Foundation of China under Grant Nos 70971007, 70701002 and 70521001, and the National Basic Research Program of China under Grant No 2006CB705503.

\*\*Email: tieqiaotang@buaa.edu.cn

© 2011 Chinese Physical Society and IOP Publishing Ltd

system, the driving resistance of each car is very complex, but we can decompose it into four parts based on Ref. [29]:

$$F'_n = F_n^{\text{rolling}} + F_n^{\text{air}} + F_n^{\text{slope}} + F_n^{\text{acceleration}}, \quad (5)$$

where  $F_n^{\text{rolling}}, F_n^{\text{air}}, F_n^{\text{slope}}, F_n^{\text{acceleration}}$  are, respectively, the rolling resistance, air resistance, slope resistance and acceleration resistance of the  $n$ th car (see Fig. 2). Here we only study the effects of  $F_n^{\text{rolling}}, F_n^{\text{acceleration}}$  on the driving behavior for simplicity, thus Eq. (5) can be rewritten as<sup>[29]</sup>

$$F'_n = F_n^{\text{rolling}} + F_n^{\text{acceleration}} = m_n g f_n + \delta_n m_n \frac{dv_n}{dt}, \quad (6)$$

where  $m_n$  is the  $n$ th car's mass,  $g$  is the gravity acceleration,  $f_n$  is the  $n$ th car's rolling resistance coefficient and  $\delta_n$  is the correction coefficient of the rotating mass. Since the FDV model did not consider driving resistance, the resultant force of the FVD model is just the driving force of the  $n$ th car. Thus, we can obtain the  $n$ th car's driving force from the FVD model,<sup>[17]</sup> based on the Newton's motion law, i.e.

$$F_n = m_n \frac{dv_n}{dt} = m_n [\kappa (V(\Delta x_n) - v_n) + \lambda \Delta v_n], \quad (7)$$

where  $\kappa$  and  $\lambda$  are the coefficients of the FVD model. The  $n$ th car's resultant force is equal to the difference between its driving force and the driving resistance, i.e.

$$F_n^{\text{resultantforce}} = F_n - F'_n. \quad (8)$$

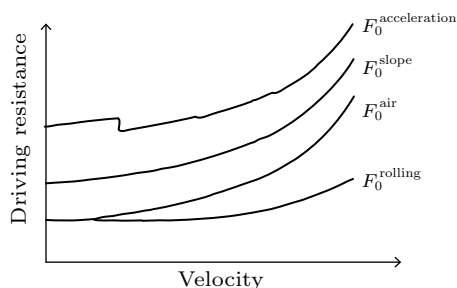


**Fig. 2.** The relationship between the driving resistance of the  $n$ th car and its velocity.<sup>[29]</sup>

Using Newton's motion law and Eqs. (6)–(8), we can immediately obtain the acceleration of the  $n$ th car, i.e.

$$\frac{d^2 x_n(t)}{dt^2} = \frac{\kappa [V(\Delta x_n) - v_n(t)] + \lambda \Delta v_n - \sigma g f_n}{1 + \delta_n}, \quad (9)$$

where  $V(\Delta x_n)$  is the optimal velocity,  $\kappa$ ,  $\lambda$  and  $\sigma$  are three car-following coefficients. Based on Ref. [17] we also set  $\kappa$  as constant and define  $\lambda$  as

$$\lambda = \begin{cases} a, & \Delta x_n \leq s_c, \\ b, & \Delta x_n > s_c, \end{cases} \quad (10)$$

where  $a$ ,  $b$  and  $s_c$  are constants,  $\sigma$  can be defined as

$$\sigma = \begin{cases} 1, & v_n > 0, \\ 0, & v_n = 0. \end{cases} \quad (11)$$

In addition, the optimal velocity  $V(\Delta x_n)$  is defined as<sup>[14]</sup>

$$V(\Delta x_n) = V_1 + V_2 \tanh [C_1(\Delta x_n - l_c) - C_2], \quad (12)$$

where  $l_c$  is the car length,  $V_1$ ,  $V_2$ ,  $C_1$ ,  $C_2$  are constants.

Based on Ref. [29] we can approximately define the parameter  $\delta_n$  as 1. The parameter  $f_n$  is often relevant to the  $n$ th car's performance and the quality of the road, but here we define it as a constant for simplicity. The parameters in Eqs. (7)–(12) have no qualitative effects on the following numerical results, so we define them as follows:

$$\begin{aligned} \kappa &= 0.41 \text{ s}^{-1}, \quad g = 9.8 \text{ m/s}^2, \quad a = 0.5, \quad b = 0, \\ s_c &= 150 \text{ m}, \quad V_1 = 6.75 \text{ m/s}, \quad V_2 = 7.91 \text{ m/s}, \\ C_1 &= 0.13 \text{ m}^{-1}, \quad C_2 = 1.57, \quad l_c = 5 \text{ m}. \end{aligned}$$

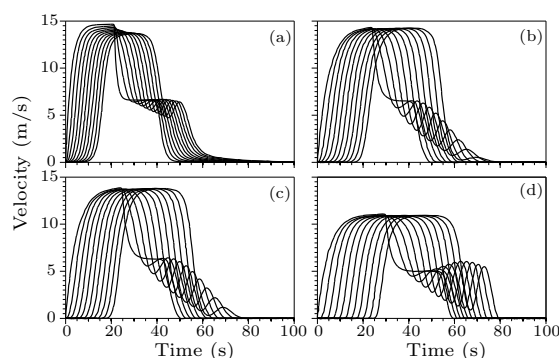


**Fig. 3.** The velocity evolution of each car: (a) FVD model, (b)  $f = 0.01$ , (c)  $f = 0.03$ , (d)  $f = 0.15$ .

In order to compare our model with the FVD model, the simulation conditions are set as: 11 cars distribute on a road, where the 11th car is at the origin and the headway of other cars is 7.4 m; there is a traffic light and a barrier on the road, where the traffic light is located at 74 m and the barrier is located at 500 m; all cars are still when  $t < 0$ ; the signal light turns green and all cars will immediately start at  $t = 0$ ; all cars will eventually stop. First, we study the evolution of the velocity of each car during the processes of the starting and braking (see Fig. 3). From this figure, we can conclude the following results: (1) Compared to the FVD model, the velocity of our model is less than that of the FVD model because the driving resistance will reduce the acceleration of each car. In addition, the reduction of the velocity will increase with the driving resistance. (2) During the braking process, the FVD model will produce three prominent phases, i.e. the velocity of each car will sharply drop in the first phase, the velocity will sharply drop again after a short fluctuation in the second phase and the

velocity will gradually drop to zero in the third phase; our model will produce the above three phases, too, but the drop trend of the velocity is more smooth, the fluctuation amplitude increases with the driving resistance and the driving resistance makes the second phase more prominent.

Using Fig. 3, we further study the delay time  $\delta t$  and the kinematic wave velocity  $c_j$  at jam density,  $\delta t$ ,  $c_j$  are often complex in the braking process and they should be demarcated by observed data, so we only list them in the starting process in this study (see Table 1). From Table 1, we find that  $\delta t$  will increase and  $c_j$  will decrease with the driving resistance.

Table 1. Delay time and kinematic wave velocity at jam density in the process of starting. FISR: frozen or impacted snow road.

Parameters	Suitable situations	$\delta t$ (s)	$c_j$ (km/h)
FVD model	Ideal road	1.4	19.03
$f = 0.01$	Asphalt or beton road	2.0	13.32
$f = 0.03$	FISR	2.1	12.69
$f = 0.15$	Muddy road	2.6	10.25

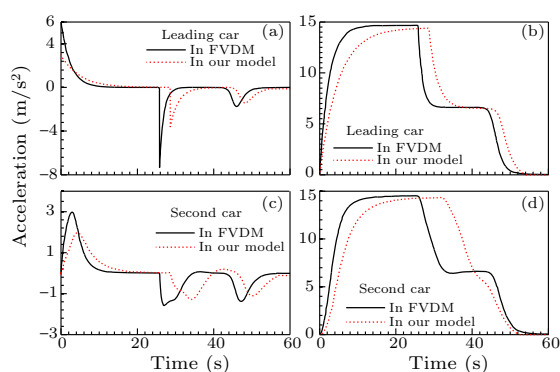


Fig. 4. The velocity and acceleration of the leading car and its following car, where  $f = 0.01$  in our model.

Next, we investigate the evolution of the velocity and acceleration of the leading car and its following car (see Fig. 4) and the motion trail of each car (see Fig. 5) during the starting and braking processes. From the two figures, we can conclude the following results: (a) During the starting process, the acceleration of our model is first lower then higher than that of the FVD model, but the two accelerations will eventually evolve into zero (see Figs. 4(a) and 4(c)); the velocity of our model is more stable than that of the FVD model (see Figs. 4(b) and 4(d)). The reasons are as follows: the cars of our model will take longer time to reach the maximum velocity than that of the FVD model, so they will still accelerate when the cars of the FVD model have already reached the maximum velocity, which leads to the acceleration of our model higher than that of the FVD model during this time; but the cars of the two models will eventually accelerate to the maximum velocity, so the accelerations of the two models will evolve into zero. (b) The driving re-

sistance has reduced the velocity, so the cars of our model will take longer time to reach the barrier than the FVD model, i.e. the braking process of our model is delayed (see Fig. 4). (c) All cars will quickly evolve into the uniform motion during the starting process; remarkable wavefronts will appear during the braking process; these wavefronts will turn more prominent and the headway of each car will gradually increase with the driving resistance (Fig. 5).

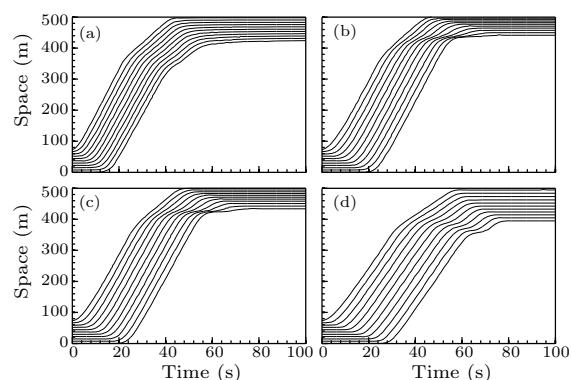


Fig. 5. The trail of each car. (a) FVD model; (b)  $f = 0.01$ ; (c)  $f = 0.03$ ; (d)  $f = 0.15$ .

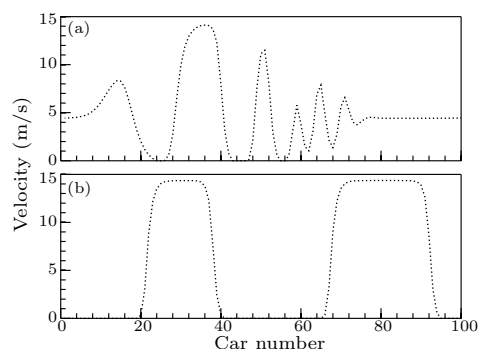


Fig. 6. The velocity of each car under the small perturbation, where (a)  $t = 150$  s and (b)  $t = 1500$  s.

Finally, we adopt periodic boundary condition to study the effect of driving resistance on the evolution of small perturbation. The initial conditions are as follows:

$$x_1(0) = 1 \text{ m}; \quad x_n(0) = (n-1)L/n, \quad \text{if } n \neq 1;$$

$$v_n(0) = V(L/n),$$

where  $N = 100$ ,  $L = 1500$  m. We here set  $\lambda = 0.5 \text{ s}^{-1}$  since the headway is very small and other parameters are the same as that of Fig. 3(b). Figure 6 is the velocity profile of each car at  $t = 150$  s and  $t = 1500$  s. From Fig. 6, we have: (1) The above perturbation will produce traffic jam phenomenon. (2) There are eventually two types of velocities in the system (Fig. 6(b)): one is approximately equal to zero; the other is approximately equal to maximum velocity. Furthermore, the two types of velocities will alternates, so the stop-and-go phenomenon will appear.

Although many traffic flow models have been developed to describe various complex traffic phenomena, they cannot reproduce the effects of driving resistance on traffic flow. In this study, we present a new car-following model which considers driving resistance. The numerical results show that our model can describe the dynamic property of each car during the processes of starting and braking. However, we assume that the driving resistant is irrelevant to the velocity. In fact, driving resistance is often very complex and depends on many factors (the velocity, the road quality), so we should further study the quantitative relation between the driving resistance and the velocity by use of many experimental data and develop a more reasonable traffic flow model to describe the effects of driving resistant on traffic flow.

## References

- [1] Chowdhury D, Santen L and Schadschneider A 2000 *Phys. Rep.* **329** 199
- [2] Helbing D 2001 *Rev. Mod. Phys.* **73** 1067
- [3] Sun X M and Dong Y J 2006 *Chin. Phys. Lett.* **23** 2494
- [4] Li K P and Gao Z Y 2004 *Chin. Phys. Lett.* **21** 1212
- [5] Yang M L, Liu Y G and You Z S 2007 *Chin. Phys. Lett.* **24** 2910
- [6] Chen T, Jia B, Li X G et al 2008 *Chin. Phys. Lett.* **25** 2795
- [7] Zhao B H, Hu M B, Jiang R and Wu Q S 2009 *Chin. Phys. Lett.* **26** 118902
- [8] Pipes L A 1953 *J. Appl. Phys.* **24** 271
- [9] Chandler R E, Herman R and Montroll E W 1958 *Oper. Res.* **6** 165
- [10] Herman R, Montroll E W, Potts R B and Rothery R W 1959 *Oper. Res.* **7** 86
- [11] Newell G F 1961 *Oper. Res.* **9** 209
- [12] Gazis D C, Herman R and Rothery R W 1961 *Oper. Res.* **9** 545
- [13] Bando M, Hasebe K, Nakayama A, Shibata A and Sugiyama Y 1995 *Phys. Rev. E* **51** 1035
- [14] Helbing D and Tilch B 1998 *Phys. Rev. E* **58** 133
- [15] Nagatani T 1999 *Phys. Rev. E* **60** 6395
- [16] Lenz H, Wagner C K and Sollacher R 1999 *Eur. Phys. J. B* **7** 331
- [17] Jiang R, Wu Q S and Zhu Z J 2001 *Phys. Rev. E* **64** 017101
- [18] Várhelyi A and Mäkinen T 2001 *Transp. Res. C* **9** 191
- [19] Hasebe K, Nakayama A and Sugiyama Y 2004 *Phys. Rev. E* **69** 017103
- [20] Ge H X, Dai S Q, Dong L Y and Xue Y 2004 *Phys. Rev. E* **70** 066134
- [21] Ahn S, Cassidy M J and Laval J 2004 *Transp. Res. B* **38** 431
- [22] Zhao X M, Gao Z Y 2005 *Eur. Phys. J. B* **47** 145
- [23] Wang T, Gao Z Y and Zhao X M 2006 *Acta Phys. Sin.* **55** 634 (in Chinese)
- [24] Han X L, Jiang C Y, Ge H X and Dai S Q 2007 *Acta Phys. Sin.* **56** 4383 (in Chinese)
- [25] Spyropoulou I 2007 *Transportmetrica* **3** 231
- [26] Gunay B 2007 *Transp. Res. B* **41** 722
- [27] Tordeux A, Lassarre S and Roussignol M 2010 *Transp. Res. B* **44** 1115
- [28] Ossen S and Hoogendoorn S P 2011 *Transp. Res. C* **19** 182
- [29] Yu Z S 2006 *Automobile Theory* 4th edn (Beijing: China Machine Press)

# Chinese Physics Letters

Volume 28

Number 3

2011

## GENERAL

- 030201** Approximate Symmetry Reduction for Initial-value Problems of the Extended KdV-Burgers Equations with Perturbation  
LI Ji-Na, ZHANG Shun-Li
- 030202** Traveling Wave Evolutions of a Cosh-Gaussian Laser Beam in Both Kerr and Cubic Quintic Nonlinear Media Based on Mathematica  
WANG Jun-Min
- 030203** Application of the CE/SE Method to a Two-Phase Detonation Model in Porous Media  
DONG He-Fei, HONG Tao, ZHANG De-Liang
- 030301** Nonlocality Sudden Birth and Transfer in System and Environment  
QIU Liang
- 030302** Quantum Secure Direct Communication with Five-Qubit Entangled State  
LIN Song, GAO Fei, LIU Xiao-Fen
- 030401** Effect of the Inverse Volume Modification in Loop Quantum Cosmology  
XIONG Hua-Hui, ZHU Jian-Yang
- 030501** Exotic Homoclinic Surface of a Saddle-Node Limit Cycle in a Leech Neuron Model  
YOOER Chi-Feng, WEI Fang, XU Jian-Xue, ZHANG Xin-Hua
- 030502** Existence of Stick-Slip Periodic Solutions in a Dry Friction Oscillator  
LI Qun-Hong, CHEN Yu-Ming, QIN Zhi-Ying
- 030503** Resonance and Rectification in a Two-Dimensional Frenkel-Kontorova Model with Triangular Symmetry  
YANG Yang, WANG Cang-Long, DUAN Wen-Shan, CHEN Jian-Min

## THE PHYSICS OF ELEMENTARY PARTICLES AND FIELDS

- 031101** Flat Currents of Green-Schwarz Superstring in  $AdS_3 \times S^3$  under Symmetry Transformations  
WANG Zhan-Yun, KE San-Min, HAO Kun, SHI Kang-Jie
- 031301** Nucleon-Nucleon Interaction in Constituent Quark Models  
XU Pu, HUANG Hong-Xia, PING Jia-Lun, WANG Fan

## NUCLEAR PHYSICS

- 032101** Benford's Law in Nuclear Structure Physics  
JIANG Hui, SHEN Jia-Jie, ZHAO Yu-Min

## ATOMIC AND MOLECULAR PHYSICS

- 033101** Fine Structures of Atomic Excited States: Precision Atomic Spectroscopy and Electron-Ion Collision Process  
GAO Xiang, CHENG Cheng, LI Jia-Ming
- 033201** Magneto-Optical Trapping of  $^{88}\text{Sr}$  atoms with 689 nm Laser  
WANG Qiang, LIN Bai-Ke, ZHAO Yang, LI Ye, WANG Shao-Kai, WANG Min-Ming, ZANG Er-Jun, LI Tian-Chu, FANG Zhan-Jun
- 033202** Modulation Transfer Spectroscopy of Ytterbium Atoms in a Hollow Cathode Lamp  
WANG Wen-Li, XU Xin-Ye
- 033301** Ultrafast Photodissociation Dynamics of the F State of Sulfur Dioxide by Femtosecond Time-Resolved Pump-Probe Method  
ZHANG Dong-Dong, NI Qiang, LUO Si-Zuo, ZHANG Jing, LIU Hang, XU Hai-Feng, JIN Ming-Xing, DING Da-Jun

(Continued on inside back cover)

- 033401 Radiative Decay of Proton Colliding with Rb at Low Energies**  
ZHOU Yu, QU Yi-Zhi, LIU Chun-Hua, LIU Xiao-Ju
- 033601 Diffusion and Interface Reaction of Cu/Si (100) Films Prepared by Cluster Beam Deposition**  
GAO Xing-Xin, JIA Yan-Hui, LI Gong-Ping, CHO Seong-Jin, KIM Hee
- FUNDAMENTAL AREAS OF PHENOMENOLOGY(INCLUDING APPLICATIONS)**
- 034101 Electromagnetic Scattering from Rough Sea Surface with PM Spectrum Covered by an Organic Film**  
WANG Rui, GUO Li-Xin, WANG An-Qi, WU Zhen-Sen
- 034201 Terahertz Generation in Nonlinear Crystals with Mid-Infrared CO<sub>2</sub> Laser**  
LU Yan-Zhao, WANG Xin-Bing, MIAO Liang, ZUO Du-Luo, CHENG Zu-Hai
- 034202 Optimization of Supercontinuum Sources for Ultra-Broadband T-CARS Spectroscopy**  
LIU Xing, LIU Wei, YIN Jun, QU Jun-Le, LIN Zi-Yang, NIU Han-Ben
- 034203 Magneto-optic Crystal Polarization Controller Assisted Mode-Locked Fiber Laser**  
ZHAO Guang-Zhen, GUI Li-Li, XIAO Xiao-Sheng, YANG Chang-Xi
- 034204 Extending the Bandwidth of Electric Ring Resonator Metamaterial Absorber**  
LUO Hao, WANG Tao, GONG Rong-Zhou, NIE Yan, WANG Xian
- 034205 Impact of Spectral Filter on Phase Modulation Pulse in Fiber Front End System**  
LI Jing, WANG Jian-Jun, XU Dang-Peng, LIN Hong-Huan, GENG Yuan-Chao, LI Ming-Zhong, DENG Ying, ZHU Na, ZHANG Rui, JING Feng
- 034206 Modified Raman Response Model and Supercontinuum Generation in Flat Dispersion Photonic Crystal Fiber with Two-Zero Dispersion Wavelengths**  
WANG He-Lin, YANG Ai-Jun, LENG Yu-Xin, WANG Cheng
- 034207 Cooperative Quantum Cutting in Er<sup>3+</sup>/Yb<sup>3+</sup> Codoped Oxyfluoride Glass Ceramics**  
LUO Shi-Qiang, ZHAO Li-Juan, HU Nan, ZHANG Ming, ZHANG Pan, WANG Ya-Zhou, YU Hua
- 034208 Enhancing the Robustness of the Microcavity Coupling System**  
YAN Ying-Zhan, JI Zhe, YAN Shu-Bin, LIU Jun, XUE Chen-Yang, ZHANG Wen-Dong, XIONG Ji-Jun
- 034209 Improved Plane-Wave Expansion Method for Band Structure Calculation of Metal Photonic Crystal**  
JIANG Bin, ZHOU Wen-Jun, CHEN Wei, LIU An-Jin, ZHENG Wan-Hua
- 034301 An Adaptive Objective Function for Evaporation Duct Estimations from Radar Sea Echo**  
ZHANG Jin-Peng, WU Zhen-Sen, WANG Bo
- 034302 Experiment Observation on Acoustic Forward Scattering for Underwater Moving Object Detection**  
LEI Bo, MA Yuan-Liang, YANG Kun-De
- 034303 Applications of Waveguide Invariant Theory to the Analysis of Interference Phenomena in Deep Water**  
LI Qian-Qian, LI Zheng-Lin, ZHANG Ren-He
- 034701 Tortuosity of Flow Paths through a Sierpinski Carpet**  
LI Jian-Hua, YU Bo-Ming
- 034702 A Mathematical Model for Studying the Slip Effect on Peristaltic Motion with Heat and Mass Transfer**  
Tasawar Hayat, Najma Saleem, Awatif A. Hendi
- 034703 Statistical Analysis of Coherent Vortical Structures in a Supersonic Turbulent Boundary Layer**  
WANG Li, LU Xi-Yun
- PHYSICS OF GASES, PLASMAS, AND ELECTRIC DISCHARGES**
- 035201 Effects of Laser Parameters on Fast Electron Generation in a Multihole Array Target**  
JI Yan-Ling, DUAN Tao, JIANG Gang, WU Wei-Dong, TANG Yong-Jian

- 035202 Self-Assembled Wire Arrays and ITO Contacts for Silicon Nanowire Solar Cell Applications**  
 YANG Cheng, ZHANG Gang, LEE Dae-Young, LI Hua-Min, LIM Young-Dae, YOO Won Jong,  
 PARK Young-Jun, KIM Jong-Min
- 035203 Time-Resolved Radiography using Chirp-Pulse Proton Beams**  
 TENG Jian, ZHAO Zong-Qing, ZHU Bin, HONG Wei, CAO Lei-Feng, ZHOU Wei-Min,  
 SHAN Lian-Qiang, GU Yu-Qiu
- CONDENSED MATTER: STRUCTURE, MECHANICAL AND THERMAL PROPERTIES**
- 036101 Growth of Zinc Blende GaAs/AlGaAs Radial Heterostructure Nanowires by a Two-Temperature Process**  
 GUO Jing-Wei, HUANG Hui, REN Xiao-Min, YAN Xin, CAI Shi-Wei, GUO Xin, HUANG Yong-Qing,  
 WANG Qi, ZHANG Xia, WANG Wei
- 036102 Wetting of Liquid Iron in Carbon Nanotubes and on Graphene Sheets: A Molecular Dynamics Study**  
 GAO Yu-Feng, YANG Yang, SUN De-Yan
- 036103 Formation and Compression Behavior of Two-Phase Bulk Metallic Glasses with a Minor Addition of Aluminum**  
 ZONG Hai-Tao, MA Ming-Zhen, ZHANG Xin-Yu, QI Li, LI Gong, JING Qin, LIU Ri-Ping
- 036104 Denuded Zone Formation in Germanium Codoped Heavily Phosphorus-Doped Czochralski Silicon**  
 LIN Li-Xia, CHEN Jia-He, WU Peng, ZENG Yu-Heng, MA Xiang-Yang, YANG De-Ren
- 036105 Influence of Oxygen in Sputtering and Annealing Processes on Properties of ZnO:Ag Films Deposited by rf Sputtering**  
 DUAN Li, GAO Wei
- 036106 Computer Simulation of the Electronic Structures and Absorption Spectra for a KMgF<sub>3</sub> Crystal Containing a Potassium Vacancy**  
 CHENG Fang, LIU Ting-Yu, ZHANG Qi-Ren, QIAO Hai-Ling, ZHOU Xiu-Wen
- 036107 First Principles Study of Dopant Site Selectivity in Ordered Perovskite CaCu<sub>3</sub>Ti<sub>4</sub>O<sub>12</sub>**  
 XU Li-Chun, WANG Ru-Zhi, DENG Yang, YAN Hui
- 036108 Deep Energy Levels Formed by Se Implantation in Si**  
 GAO Li-Peng, HAN Pei-De, MAO Xue, FAN Yu-Jie, HU Shao-Xu, ZHAO Chun-Hua, MI Yan-Hong
- 036201 Critical Free Volume Concentration of Shear Banding Instability in Metallic Glasses**  
 LIU Long-Fei, CAI Zhi-Peng, LI Hui-Qiang, ZHANG Guang-Ye, GUO Shi-Bo
- 036401 Isotropic Thermal Expansivity and Anisotropic Compressibility of ReB<sub>2</sub>**  
 LIU Xi, LIU Wei, HE Qiang, DENG Li-Wei, WANG He-Jin, HE Duan-Wei, LI Bao-Sheng
- 036801 Epitaxial Growth of Si(111)/Er<sub>2</sub>O<sub>3</sub> (111) Structure on Si(111) by Molecular Beam Epitaxy**  
 XU Run, TANG Min-Yan, ZHU Yan-Yan, WANG Lin-Jun
- CONDENSED MATTER: ELECTRONIC STRUCTURE, ELECTRICAL, MAGNETIC, AND OPTICAL PROPERTIES**
- 037101 Electronic Structure and Optical Properties of Layered Ternary Carbide Ti<sub>3</sub>AlC<sub>2</sub>**  
 JIANG Jiu-Xing, JIN Shan, WANG Zhen-Hua, TAN Chang-Long
- 037102 Cathodoluminescence of Yellow and Blue Luminescence in Undoped Semi-insulating GaN and n-GaN**  
 HOU Qi-Feng, WANG Xiao-Liang, XIAO Hong-Ling, WANG Cui-Mei, YANG Cui-Bai, YIN Hai-Bo,  
 LI Jin-Min, WANG Zhan-Guo
- 037103 Exchange Enhancement of Spin-Splitting in Al<sub>x</sub>Ga<sub>1-x</sub>N/GaN Heterostructures in Tilted Magnetic Fields**  
 TANG Ning, HAN Kui, LU Fang-Chao, DUAN Jun-Xi, XU Fu-Jun, SHEN Bo



- 037201 Simultaneous Enhancement of Electrical Conductivity and Seebeck Coefficient of Poly(3,4-ethylenedioxythiophene):Poly(styrenesulfonate) Films Treated with Urea**  
KONG Fang-Fang, LIU Cong-Cong, XU Jing-Kun, JIANG Feng-Xing, LU Bao-Yang, YUE Rui-Rui, LIU Guo-Dong, WANG Jian-Min
- 037401 Coupling of a  $Tl_2Ba_2CaCu_2O_8$  Thin Film Intrinsic Josephson Junction and a Fabry–Perot Resonator**  
FAN Bin, WANG Zheng, YUE Hong-Wei, YAN Shao-Lin, JI Lu, HE Ming, SONG Feng-Bin, FANG Lan, ZHAO Xin-Jie
- 037501 Noncollinear Magnetism Calculation of Iron Clusters with Spin-Orbit Coupling**  
CHENG Zhi-Da, ZHU Jing, TANG Zheng
- 037601 Electron Paramagnetic Resonance and Optical Absorption of  $VO^{2+}$  Doped Ammonium Selenate Single Crystals**  
Ram Kripal, Ashutosh Kumar Shukla
- 037701 Microwave Absorption Properties of Ni-Foped SiC Powders in the 2–18 GHz Frequency Range**  
JIN Hai-Bo, LI Dan, CAO Mao-Sheng, DOU Yan-Kun, CHEN Tao, WEN Bo, Simeon Agathopoulos
- 037702 Enhanced Ferromagnetism and Microwave Dielectric Properties of  $Bi_{0.95}Y_{0.05}FeO_3$  Nanocrystals**  
HOU Zhi-Ling, ZHOU Hai-Feng, YUAN Jie, KANG Yu-Qing, YANG Hui-Jing, JIN Hai-Bo, CAO Mao-Sheng
- CROSS-DISCIPLINARY PHYSICS AND RELATED AREAS OF SCIENCE AND TECHNOLOGY**
- 038101 Fabrication of a Polymer Micro Needle Array by Mask-Dragging X-Ray Lithography and Alignment X-Ray Lithography**  
LI Yi-Gui, YANG Chun-Sheng, LIU Jing-Quan, SUGIYAMA Susumu
- 038401 Intermediate-Band Solar Cells Based on InAs/GaAs Quantum Dots**  
YANG Xiao-Guang, YANG Tao, WANG Ke-Fan, GU Yong-Xian, JI Hai-Ming, XU Peng-Fei, NI Hai-Qiao, NIU Zhi-Chuan, WANG Xiao-Dong, CHEN Yan-Ling, WANG Zhan-Guo
- 038501 A Room-Temperature Pre-calibration Procedure for Gradiometer Sifting**  
ZHANG Shu-Lin, LIU Yang-Bo, LIU Ming, WANG Yong-Liang, KONG Xiang-Yan, XIE Xiao-Ming
- 038801 Hierarchical Porous Carbon Counter Electrode for Dye-Sensitized Solar Cells**  
WANG Gui-Qiang, HUANG Cong-Cong, XING Wei, ZHUO Shu-Ping
- 038901 Size Dependency of Income Distribution and Its Implications**  
ZHANG Jiang, WANG You-Gui
- 038902 A New Car-Following Model with Consideration of Driving Resistance**  
LI Chuan-Yao, TANG Tie-Qiao, HUANG Hai-Jun, SHANG Hua-Yan
- GEOPHYSICS, ASTRONOMY, AND ASTROPHYSICS**
- 039401 Diffusion Simulation of Outer Radiation Belt Electron Dynamics Induced by Superluminous L-O Mode Waves**  
XIAO Fu-Liang, HE Zhao-Guo, ZHANG Sai, SU Zhen-Peng, CHEN Liang-Xu
- 039601 Numerical Validation and Comparison of Three Solar Wind Heating Methods by the SIP-CESE MHD Model**  
YANG Li-Ping, FENG Xue-Shang, XIANG Chang-Qing, JIANG Chao-Wei
- 039701 A Constraint of Black Hole Mass and the Inner Edge Radius of Relativistic Accretion Disc**  
HE Liang, HUANG Chang-Yin, WANG Ding-Xiong
- 039801 An Interacting Two-Fluid Scenario for Dark Energy in an FRW Universe**  
Hassan Amirhashchi, Anirudh Pradhan, Bijan Saha